

*Citation for published version:*

Lv, X, Gu, C, Liu, X & Weng, Y 2016, 'Effect of gasified biomass fuel on load characteristics of an intermediate-temperature solid oxide fuel cell and gas turbine hybrid system', *International Journal of Hydrogen Energy*, vol. 41, no. 22, pp. 9563-9576. <https://doi.org/10.1016/j.ijhydene.2016.04.104>

*DOI:*

[10.1016/j.ijhydene.2016.04.104](https://doi.org/10.1016/j.ijhydene.2016.04.104)

*Publication date:*

2016

*Document Version*

Peer reviewed version

[Link to publication](#)

*Publisher Rights*

CC BY-NC-ND

**University of Bath**

**Alternative formats**

If you require this document in an alternative format, please contact:  
[openaccess@bath.ac.uk](mailto:openaccess@bath.ac.uk)

**General rights**

Copyright and moral rights for the publications made accessible in the public portal are retained by the authors and/or other copyright owners and it is a condition of accessing publications that users recognise and abide by the legal requirements associated with these rights.

**Take down policy**

If you believe that this document breaches copyright please contact us providing details, and we will remove access to the work immediately and investigate your claim.

# Effect of gasified biomass fuel on load characteristics of an intermediate-temperature solid oxide fuel cell and gas turbine hybrid system

Xiaojing Lv<sup>a</sup>, Chenghong Gu<sup>b</sup>, Xing Liu<sup>a</sup>, Yiwu Weng<sup>a,\*</sup>

<sup>a</sup> Key Laboratory for Power Machinery and Engineering of Ministry of Education, School of Mechanical Engineering, Shanghai Jiao Tong University, Shanghai 200240, China

<sup>b</sup> Department of Electronic and Electrical Engineering, University of Bath, Bath, BA2 7AY, UK

---

## Abstract

This work uses the mathematical model of an intermediate-temperature solid oxide fuel cell and gas turbine (IT-SOFC/GT) hybrid system to study the effects of gasified biomass fuels on system load characteristics. The system performance is investigated by using four types of fuels in each adjusting mode. The relation between the fuel type and load adjusting mode is obtained for users and designers to select the appropriate fuel for reasonable operation modes. Results show that the hybrid system of 182.4kW has a high electric efficiency of 60.78% by using wood chip gas (WCG). If cotton wood gas (CWG) and corn stalk gas (CSG) are used, both boundary values of steam to carbon ratio ( $S/C_{bv}$ ) and system power are higher, but system efficiencies decrease to 57.36% and 57.87% respectively. In the designed three load adjusting modes, the system can reach maximum efficiency over 59% with four types of biomass gases. If high efficiency and a wide range of load adjustment are required, users can select Case B to use fuels like WCG and GSG. When higher efficiency and low load is expected, Case A is more desirable. With fuels like CWG and CSG, the system has good safety performance in Case C.

---

\*Corresponding author. Tel.: +86 21 3420 6342; fax: +86 21 3420 6342.  
E-mail address: ywweng@sjtu.edu.cn.

**Keywords:** intermediate temperature solid oxide fuel cell; gas turbine; hybrid system; gasified biomass gas; load characteristic; adjusting mode

---

## 1. Introduction

Solid oxide fuel cell and gas turbine (SOFC/GT) hybrid systems are thought to be the most attractive energy conversion systems in future energy markets because of high efficiency, low pollution, and fuel flexibility (such as natural gas, biomass gas) [1,2]. Biomass is rich and important renewable energy and it has the characteristics of low net CO<sub>2</sub> emission rate and SO<sub>2</sub> emission rate. For this reason, biomass fuelled SOFC/GT hybrid systems are regarded as one of the most promising power generation equipment [3,4].

In recent years, some theoretical and experimental research has been carried out in the integrated systems based on biomass gasification and SOFC/GT systems [5-9]. These works mainly focus on system modeling [5,6], integration and optimization design [7,8], and selection and impact analysis of component operation parameters [9], providing the basis for utilizing biomass gas in hybrid systems. Unlike fossil fuels, the components and quality of biomass gas fuels are mainly affected by gasification process, process control parameters and raw materials [10]. In biomass gasification, fuel compositions depend on the gasification agent. For example, the concentrations of H<sub>2</sub>, CH<sub>4</sub>, CO, and N<sub>2</sub> vary greatly when oxygen, air, or steam is used as gasification agent [10,11].

However, the variation of fuel type (or composition) has a great impact on system performance. The main reasons are as follows: 1) fuel cell electrochemical reaction is mainly affected by temperature and fuel composition, and the composition variation will cause a large

fluctuation in fuel cell performance [10]; 2) Reforming reactions in reformers are reversible thermodynamic equilibrium [12], which will occur automatically due to the changes in fuel compositions; 3) The combined effect of the previous two factors can cause changes in the thermodynamic performance of other components, and the design and layout of hybrid systems.

Magistri.et.al [13] showed that when the designed fuel  $\text{CH}_4$  was completely replaced by synthetic gas and biomass gas, system efficiency decreased from 61.7% to 53.5% and 49.2% respectively, and the selection of parameters for gas turbines and injector should also be changed. Santin.et.al [14,15] investigated the SOFC/GT hybrid system with two liquid fuels (methanol and kerosene) and developed four layouts by considering different fuel processing strategies. They also conducted thermodynamic and investment analysis for the hybrid system. Van herle.et.al [16] studied a process flow model of an SOFC system supplied with sewage biogas. For partial oxidation of biogas or pure hydrogen feeding, **electric efficiency** dropped under 43%. Zabihian.et.al [10] compared the output power, specific work, and efficiency of the SOFC/GT hybrid system fueled with methane and **various types of biomasses**. Zabihian.et.al [17,18] further investigated the effect of fuel composition on the hybrid system performance from the perspective of inlet fuel energy content. Sucipta.et.al [19] found that the change of  $\text{H}_2\text{O}$  and  $\text{H}_2$  concentration in fuel from 0% to 50% slightly reduced the efficiency of hybrid systems. An increase of CO concentration produced similar effects as that of  $\text{CO}_2$  and resulted in a decreasing efficiency of both SOFC module and hybrid system significantly. Sucipta.et.al [20] analyzed the **electric performance** of a biomass SOFC/GT hybrid system by comparing typical air, oxygen, and steam-blown biomass gasification processes. Results showed that the

electric efficiencies of the three biomass fuel cases were lower than that of pure methane case. Rokni.et.al [21] showed that the electric efficiency of a hybrid SOFC-Stirling plant was 60%. With a slight decrease in fuel utilization factor, the power of Stirling engine was found to increase. By lowering SOFC working temperature, the plant efficiency decreased for all fuels except ammonia. Similar research could be found in [22-25].

All previous work has identified the change of fuel type and composition to be important factors for a hybrid system at designed condition. However, the hybrid system is a strongly-coupled thermoelectric system. With different types of inlet fuels, there are some important issues will appear when the system operates under variable conditions due to the constraints of component matching and characteristic parameters. For example, the issues could be the influence of changes in fuel type on variable load operation and safety issues of a hybrid system, and the coupling relationship between different types of fuels and various operations. But, research in this field is very limited. Weng [26] studied the performance of a hybrid system using  $\text{CH}_4$ ,  $\text{H}_2$  and ethanol as fuel. It was found that when the hybrid system operated with  $\text{H}_2$ , the net power output at the design point decreased to 70% of the  $\text{CH}_4$ , while the design net efficiency dropped to 55%. Similar to  $\text{H}_2$ , the net output power of the ethanol-fueled system fell below 88%.

Based on the previous research, this work studies the operating characteristics of the main components (such as fuel cell, gas turbine, and reformer) of a hybrid system and its variable load characteristics under design and off-design conditions, when the system is fueled with different types of gasified gases. Then, the matching relationships between load adjusting mode

and fuel type are obtained by analysis and comparison. The results are very beneficial for designers and users to select the most appropriate fuels for reasonable operation of a hybrid system.

## **2. IT-SOFC/GT calculating method and parameter selection**

### **2.1 IT-SOFC/GT hybrid system structure**

A schematic of the IT-SOFC/GT hybrid system is shown in **Fig. 1**, which mainly includes IT-SOFC, single-shaft GT, external reformer, catalytic combustor (CC), fuel compressor, water syringe pump, generator, and other components. To avoid carbon deposition, water is added for maintaining the ratio of steam to carbon [16,27] by adjusting valve 1. To prevent seal and vibration caused by the pressure difference between anode and cathode in the fuel cell [28], biomass gas needs to be compressed by a fuel compressor before entering the fuel cell for electrochemical reaction, which is adjusted by valve 2. The airflow is controlled by GT adjustment system, and the rotational speed of GT is controlled by generator equipment. Air pressurized by the compressor is heated by heat exchangers (HE) 1 and 2, which then enters the SOFC cathode to provide  $O_2$  for electrochemical reaction. Water is first heated in the evaporator to be converted into steam and then mixed with biomass gas in the mixer. The mixed gas enters the reformer after being heated by HE 1. Reformed gas enters the anode of the fuel cell to provide  $H_2$ . The unreacted fuel from the SOFC anode will be completely combusted in the CC. High-temperature gas enters the turbine to generate power after heating air. The exhaust gas of the turbine preheats fuel and air, and then heats the evaporator before being released into the atmosphere.

## 2.2 IT-SOFC/GT hybrid system modeling

The mathematical model of the IT-SOFC/GT was described in detail in the previous literature [29,30]. All important equations of this model are shown in appendix A. The modeling approach, mathematical formula, specific geometric parameters, physical parameters, and operating conditions can be found in the literature [29,30].

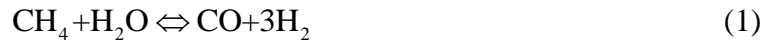
In this paper, the anode-supported IT-SOFC (873–1073 K) developed by Aguiar [31] is used to fit into the hybrid system. The 2D fuel cell model includes an electrochemical model and a thermodynamic model based on mass and energy balance equations from Eqs (1)~(19), as shown in Table A. The electrochemical model describes the function relation between fuel cell voltage, various polarization losses, and current density. It considers not only the influence of ohm, activation and concentration polarization losses on the Nernst potential, but also the changes in gas composition caused by the electrochemical reaction and changes in specific heat value caused by temperature variations. The fuel cell stack is assumed to have 912 planar fuel cells, providing 144 kW power. Its working temperature, average current density, and fuel utilization are chosen to be 1,073 K, 5,000 A/m<sup>2</sup>, and 75%, at the design condition respectively.

The gas turbine model is mainly composed of a centrifugal compressor and radial turbine. It is represented by the characteristic maps of compressor and turbine shown in Figs. 2 and 3 in [26, 30-31]. According to similarity theory, the characteristic curves of compressor and turbine can be described by a set of functions with reduced parameters from Eqs (20)~(25, as shown in Table A). For the compressor, surge boundary line is important. Therefore, the distance between surge boundary and working point is measured by surge margin (SM). When SM is smaller, the

compressor is easier to surge and the formulas are presented in [30].

The reforming model is established according to Gibbs free energy thermodynamic equilibrium reaction, mainly including strong endothermic steam reforming reaction (1) and weak exothermic water gas shift reaction (2). Six type flows of CH<sub>4</sub>, H<sub>2</sub>, CO, CO<sub>2</sub>, H<sub>2</sub>O, and N<sub>2</sub> in the reforming model can be calculated by the equilibrium Eqs. (3) and (4). H<sub>2</sub> flow before entering SOFC can be calculated by Eq. (5).

In reforming process, the S/C ratio (the ratio of steam to CH<sub>4</sub>, CO, and CO<sub>2</sub>) is an important parameter to avoid carbon deposition [32]. The boundary value of the S/C ratio (S/C<sub>bv</sub>) is dependent on the reaction temperature [16], where the detailed formula is also presented.



$$K_1 = [\text{CO}][\text{H}_2]^3 / [\text{CH}_4][\text{H}_2\text{O}] = (n_{\text{CO}} + x - y)(n_{\text{H}_2} + 3x + y)^3 / (n_{\text{CH}_4} - x)(n_{\text{H}_2\text{O}} - x - y)(n_{\text{H}_2} + 2x)^2 \quad (3)$$

$$K_2 = [\text{CO}_2][\text{H}_2] / ([\text{CO}][\text{H}_2\text{O}]) = (n_{\text{CO}_2} + y)(n_{\text{H}_2} + 3x + y) / [(n_{\text{CO}} + x - y)(n_{\text{H}_2\text{O}} - x - y)] \quad (4)$$

$$n_{\text{H}_2, \text{tot}} = n_{\text{H}_2, \text{in}} + n_{\text{CO}, \text{eq}} + 3n_{\text{CH}_4, \text{eq}} \quad (5)$$

The hybrid system also includes other components, such as CC, HE, mixer, and syringe pump. The establishment of the models and parameters selection can be found in [26,33]. This work assumes that unreacted fuel is completely combusted in the CC.

The hybrid system electric efficiency is:

$$\eta_{\text{HS}} = \frac{P_{\text{SOFC}} \times \eta_{\text{DC/AC}} + (P_{\text{T}} - P_{\text{C,air}}) \eta_{\text{g}} \times \eta_{\text{m}} - (P_{\text{C,fuel}} / \eta_{\text{e}}) - (P_{\text{P,water}} / \eta_{\text{e}})}{(y_{\text{CH}_4}^0 \times \text{LHV}_{\text{CH}_4}^0 + y_{\text{H}_2}^0 \times \text{LHV}_{\text{H}_2}^0 + y_{\text{CO}}^0 \times \text{LHV}_{\text{CO}}^0) \times M_{\text{fuel}}} \quad (6)$$



### 2.3 IT-SOFC/GT hybrid system calculation

Considering the thermal coupling between components and their safety constraints, a reasonable and scientific calculation flowchart is important for analyzing the operating performance of components and the variable load characteristics of the hybrid system. The calculation flowchart of IT-SOFC/GT is shown in Fig. 2.

The proposed system mainly uses the following three functional models to calculate and distinguish system circulation features: 1) thermodynamic calculation and component parameter matching, 2) the self-estimation of main components, 3) iteration cycle and matching of the whole system. The hybrid system is simulated in MATLAB/SIMULINK. The reforming equilibrium reactions are solved using MATLAB programming, and the component estimation modules are realized by user-defined functions.

The hybrid system is very complicated and its performance depends on many influencing factors. Apart from  $H_2$ , CO also participates in the electrochemical reaction, but its impact on the hybrid system is far less than those of other factors. Additionally, a large number of system integration and parameter variables make the thermodynamic calculation complex and difficult. Hence, for simplicity purposes, some assumptions are made [2, 10, 28]: 1) In the SOFC, only  $H_2$  participates in the electrochemical reaction, and the electrochemical reaction of CO is not considered; 2) The hybrid system has zero leakage; 3) The output temperatures of the fuel cell and reformer are their reaction temperatures; 4) Heat and pressure losses of components are constants in operation conditions; 5) The operating voltage of each cell in stack is constant.

### 2.4 Determination for fuel and load adjusting mode

In this work, gasified wood chip gas (WCG) is used for the original system design, and other three types of gasified biomass - cotton wood gas (CWG), grape seed gas (GSG) and corn stalk gas (CSG) are selected for comparison and analysis. The composition and lower heating value of gasification gases are shown in Table.1. The fuel composition is the experimental results from a two-stage gasification developed by the Institute of Thermal Engineering, Shanghai Jiao Tong University [34]. In air blown gasification process, pyrolysis zone and gasification zone are independent, making the system simple and flexible and desirable completion of pyrolysis, partial oxidation, and tar elimination. More information about the gasification can be found in [34]. Gasified gas usually contains some impurities, but the impure tar, particles, and  $H_2S$  in the gasified biomass gas in this study are assumed to be removed well in the purifying process. Thus, the effect of poison on the components or the system can be neglected.

For variable load operation of a multi-hundred kW-class SOFC/GT hybrid system, two types of load adjusting modes were proposed in previous studies: the fuel only adjusting mode and rotational speed adjusting mode [35-36]. In variable load operations, the fuel cell working temperature should be maintained close to its design value in order to reduce the decreasing extent of system efficiency. Hence, in this study, the following three types of load adjusting modes (Case A, Case B, and Case C) are adopted, and their fuel utilization factors for different inlet fuels are assumed to be constant. The three models are defined as follows, and the operating trajectories of the gas turbine are shown in Fig. 3.

Case A: Adjusting fuel proportionally and then adjusting the air to keep fuel cell working

temperature constant.

Case B: Adjusting the fuel but keeping the air constant.

Case C: Adjusting the fuel and air simultaneously to keep the fuel-air ratio constant.<sup>3</sup>

### **Performance analysis of IT-SOFC/GT at design condition**

It is important to note that, for different types of inlet fuels, fuel flow needs to be recalculated before entering the hybrid system in order to maintain the SOFC working temperature constant. When using WCG and GSG, the system operation performance can be fulfilled by purely changing fuel flow with constant  $U_f$ , 75%. However, it does not work for CWG and CSG, because that the heating values of these two fuels are lower. More seriously, increasing the fuel flow to meet fuel cell operating requirement will lead the compressor operating point to deviate into high pressure and low air flow zone, causing compressor surge and unstable operation. Hence, decreasing the  $U_f$  from 75% to 60% is used to satisfy the safe operation for the system when using CWG and CSG.

The operation performance at designed condition is obtained by using above established IT-SOFC/GT mathematic models, as shown in Table 2. It can be observed that when using the designed fuel WCG, the fuel flow rate is 2.269 mol/s, and all characteristic parameters of main components meet the requirements in Table 3 in [29]. Furthermore, the fuel cell operating parameters coincide with the results from reference [31]. For the small power system designed in this work, the electrical efficiency is 60.78%. It is noted that the catalytic combustor temperature is not more than 1200K and changes homogeneously, causing  $\text{NO}_x$  emission to be very low (nearly zero) [33] and CO to be converted into  $\text{CO}_2$  completely. Above results show

that the hybrid system has good emission and operation performance.

Notably that, for using non-design fuel, both the fuel flow rate and the current density are higher than those of the design fuel. More importantly, when using CWG and CSG,  $S/C_{bv}$  and the fuel cell voltage drop, the output power of fuel cell and GT are higher, leading the system power to increase but the efficiencies to decrease to 57.36% and 57.87% respectively. In addition, compressor consumption power increases significantly and is approximately 2 times of that of the design fuel WCG, which needs the turbine to generate more power to meet the system demand. However, for using GSG,  $S/C_{bv}$  increases and the fuel cell voltage decreases, both the power and efficiency of the hybrid system are lower than those of design fuel. The main reason is that the drop in the fuel cell power is higher than the rise in GT power.

It is also observed that all turbine inlet temperatures (TITs) are less than 1173K when using non-design fuels and the GT output powers are higher than that of designed value. This is due to the impact that the increasing fuel flow on the GT output power is greater than that of decreasing TIT.

#### **4. Analysis of the variable load characteristics of the hybrid system.**

##### **4.1 Variable load characteristics of the hybrid system in Case A**

In this mode, the fuel flow increases from 0.4 times of the design value to 1.05 times proportionally, and the air flow is controlled by adjusting the rotational speed of the gas turbine. For variable rotational speed, in order to make each operating point have a maximum value of surge margin, the operating trajectory of the gas turbine is obtained (depicted in light blue heavy line ) in Fig.3. The purple heavy line stands for the operating trajectory for the gas

turbine using CWG and CSG as fuel.

Fig. 4 (a) shows that for different inlet biomass types, both fuel flow and air flow increase with increasing system load. Note that for using WCG and GSG, the fuel flow rates are nearly equal, but are less than those of CWG and CSG. On the other hand, their corresponding air flows are greater than those of CWG and CSG. Meanwhile, for using WCG and GSG, when the gas turbine is operated at the same rotational speed, the compressor pressure is also less than that of CWG and CSG, causing the compressor operating point to drift away from surge boundary line and the surge margin to increase. As shown in Fig. 4 (a), for using WCG and GSG, the SM is higher than that of other two types of fuels when the system load increases from 46% to 80%. With increasing system load, the SM for four types of fuels has a downward trend. It can also be found that the system load changes from 40% to 103% of the rated power when using WCG and GSG, but for other two fuels, the system load ranges are 46.6% ~118.90% and 47.97%~121.12%, respectively.

Fig. 4 (b) shows that with increasing system load, the fuel cell working temperature is constant and its mean temperature gradient increases, but the voltage drops. The mean temperature gradients are higher than those of other two fuels when using WCG and GSG. More importantly, when the system uses WCG, the fuel cell voltage is the highest, followed by that of using GSG.

With increasing system load, the fuel cell output power increases but its efficiency declines, as shown in Fig.4(c). For WCG, though the fuel cell efficiency is higher than that of other fuels, it decreases from 53.73% to 47.69%. CSG fuel can make the fuel cell have a wider

and higher load adjusting range increasing from 75.85 kW to 172.32 kW, but cause its efficiency to decrease from 52.24% to 44.62%. This is because, in order to keep fuel cell temperature constant, the too low heating value of CSG makes the current density and fuel flow rate both increase and the voltage decrease. This combined effect causes the increasing extent of fuel cell power to be less than that of the heat value of the fuel entering the system, and the ultimate consequence is the decreasing cell efficiency.

In reforming process, the increasing reaction equilibrium constant  $K_1$  means that the forward reaction is performed, vice versa. Fig. 4(d) shows that with increasing system load,  $K_1$  decreases,  $K_2$  increases, and  $S/C_{bv}$  also increases. When using WCG,  $K_1$  is higher than that of GSG, and is lower than those of other two fuels. However,  $S/C_{bv}$  is less than that of GSG and is higher than those of other two fuels. This is mainly because the too low heating values of CWG and CSG make the fuel flow increase greatly. The remaining fuel after electrochemistry reaction will be combusted completely in the CC, triggering the reformer inner temperature to increase, and finally  $K_1$  to increase and both  $K_2$  and  $S/C_{bv}$  to decrease. Thus, it can be seen that high fuel flow, caused by low heating values of fuels, is beneficial for improving the reforming characteristics and safety of the reformer by reducing  $U_f$ .

In Fig. 4 (e), with increasing system load, TIT changes a little due to the limitation from constant SOFC working temperature. For using CWG as fuel, TIT is higher than that of other three fuels- CSG, WCG, and GSG. This influence trend is similar to that of the reformer. It can also be found that when using WCG and GSG, the gas turbine output power reaches the maximum value at the designed point and then declines. Using other two fuels, the gas turbine

output power is higher than those of WCG and GSG, but no maximum value exists. This further proves that gas fuels of CWG and CSG with low heating value can improve the workability of the gas turbine by reducing  $U_f$ . However, more attentions should be paid to the effect of higher gas flows on the turbine flow characteristics in this case.

Fig. 4(f) shows that with increasing system load, the hybrid system efficiency initially keeps unchanged, then reaches the maximum value at the designed point. By contrast,  $P_{GT}/P_{SOFC}$  initially increases gradually and reaches the maximum value at the design point. This is because, with constant SOFC working temperature, the system fuel-air ratio decreases due to the compressor operating characteristics, which leads to a decrease in system thermodynamic performance and finally causes the decrease in system efficiency. Although the fuel cell power and GT power both increase, the increasing level of gas turbine power is higher than that of the fuel cell, results in increasing  $P_{GT}/P_{SOFC}$ . More importantly, the system efficiency is highest when using WCG.

#### 4.2 Variable load characteristics of the hybrid system in Case B

In this case, the fuel flow is adjusted from 0.3 to 1.3 times of the designed value, and the compressor operates at designed state, as shown by the pink dot in Fig.3. The component characteristics and system performance in variable load operations with different inlet fuels are shown in Fig.5.

When the system operates in this case, the variation trends of different biomass gases are almost similar to that in Case A. The difference is that the air flow is constant and the SM is almost 16.88%, as shown in Fig.5(a). The system load changes from 17% to 134% of the rated

power when using WCG and GSG. However, for other two fuels, the system load changes from 21.96% to 153.94% and from 23.23% to 156.89%, respectively.

Fig. 5(b) shows that with increasing system load, both fuel cell working temperature and voltage increase while the cell mean temperature gradient has a minimum value. In the low load condition, the variation trend of fuel cell working temperature appears to overlap with each other, but with load increasing to 53%, the fuel cell working temperatures with using WCG and GSG are higher than those of other two fuels. In the whole load variation process, for using WCG and GSG, the voltage is higher than those of other two fuels. Meanwhile, in the low load condition, the mean temperature gradient is higher for the first two fuels, but when the load reaches rated state, the mean temperature gradients for all four fuel types are mostly identical to 6.58K/cm.

In Fig.5 (c), with increasing system load, the slope of fuel cell output power first increases and then declines, while the increasing slope of cell efficiency keeps constant. For using WCG, the cell efficiency increases from 20.37% to 50.12%, which is higher than those of other three fuels. While for CSG, the cell out power increases from 26.68 kW to 225.5 kW and the efficiency increases from 24.18% to 47.17%, which presents a wide range of high load adjustment. The main reason is that keeping air flow constant and increasing fuel flow will cause the cell working temperature to rise, and thus the combined increase of current density and voltage leads the fuel cell power to rise greatly. However, this benefit is obtained by reducing fuel utilization and increasing current density, hence the fuel cell efficiency is less than that of WCG.



With increasing system load,  $K_1$  rises, but  $K_2$  and  $S/C_{bv}$  both decrease, as shown in Fig.5(d). This is mainly because increasing fuel flow rises the reformer inner temperature, which can promote the  $CH_4$  reforming in a forward direction due to its endothermic characteristic. Thus, this can finally cause  $K_1$  to rise. While  $K_2$  declines, because of the exothermic characteristic of water, gas shift reaction and increasing temperature promotes reverse reaction. Rising temperature can effectively prevent carbon deposition at least in theory, which leads to the decrease of  $S/C_{bv}$ . Most notably that when using WCG,  $K_1$  is the highest and  $S/C_{bv}$  is the smallest. It is thus clear that the biomass gas CWG and CSG with low heating value after reducing  $U_f$  have little impact on enhancing the reforming characteristics of the reformer.

It can be seen from Fig.5(e) that, TIT and GT output power both increase with rising system load. The reason is that, by keeping air flow constant and increasing fuel flow to raise fuel-air ratio, the combustible component entering the CC increases after the electrochemical reaction, leading to increasing TIT. The combined increase of inlet temperature and gas flow entering the turbine leads the GT power to rise greatly. This trend can also be seen from the changing slopes of GT power and TIT. It is important to note that, for using WCG and GSG, TITs are higher than those of other two fuels, but the powers are less. This is because, for using other two fuels, the impacts of increasing fuel flow on the GT are higher than that of decreasing TIT, which leads the GT output power to be higher.

Fig.5 (f) shows that with increasing system load, the hybrid system efficiency increases and  $P_{GT}/P_{SOFC}$  declines. When using WCG, the system efficiency is the highest, but  $P_{GT}/P_{SOFC}$  is

the smallest. The system efficiency changes greatly when the system load is lower than 55%, and it is relatively flat when load is higher than 55% because the fuel cell is a major power component of the hybrid system. Thus, when fuel flow is small,  $P_{GT}/P_{SOFC}$  is large, and when fuel flow is high,  $P_{GT}/P_{SOFC}$  decreases. These features reflect the advantages of the fuel cell.

#### 4.3 Variable load characteristics of the hybrid system in Case C

In this mode, the fuel flow is adjusted according to the constraint of a constant fuel-air ratio and the compressor operating trajectory is shown by the green heavy line in Fig.3.

Fig.6 shows the variable load characteristics of the hybrid system in Case C. Fig.6 (a) illustrates, as the system load rises, both biomass flow and air flow increase linearly but the compressor SM decreases from 21.12% to 16.12%. This is because, with increasing rotational speed, airflow, and pressure ratio, the operating point moves up gradually close to the surge line along  $\beta$  line, causing SM to decline. It can also be seen that, when using WCG and GSG, the system load varies between 45% and 103% of the rated power, but for other two fuels, the system load ranges are 51.62%~118.56% and 52.74%~120.84%, respectively.

For a constant  $U_f$ , increasing fuel flow can escalate current density, causing more electrochemical reaction. In this process, the fuel cell working temperature first decreases to the designed value and then increases, as shown in Fig.6 (b). The fuel cell mean temperature gradient increases and voltage declines with the increasing system load. When using WCG and GSG, the fuel cell operating parameters are all higher than those of other two fuels. Fig.6 (c) shows that with increasing system load, the cell output power rises and the efficiency declines. With using WCG, the cell efficiency drops from 53.81% to 48.11%, but it is still higher than

those of other three fuels. This trend is similar to that in Fig.4 (c). However, for the reforming characteristics, when using WCG and GSG,  $K_1$  declines and  $K_2$  rises,  $S/C_{bv}$  reaches a maximum value at the design point and then declines with increasing system load. For using CWG and CSG,  $S/C_{bv}$  reaches a maximum value at 115% load condition shown in Fig.6 (d). Meanwhile, for WCG,  $K_1$  is higher than that of GSG, but it is less than those of other two fuels while the variation trend for  $S/C_{bv}$  is right opposite.

With increasing system load, TIT first decreases to the design value and then increases, the GT output power reaches a maximum value at the design point and then declines, as shown in Fig.6 (e). The difference from Cases A and B is that when the system uses CWG as fuel, the TIT is the highest. It can also be seen that, when the system operates at low load state, the GT output power is higher than those of other two fuels if WCG and GSG are used. However, rising system load can greatly increase the GT power of other two fuels, higher than those from WCG and GSG.

In Fig.6 (f), with increasing system load, the system efficiency has no significant change until it reaches the designed point, and  $P_{GT}/P_{SOFC}$  increases gradually and reaches a maximum value at the designed point. This is because when the system is in a light load state, low rotational speed leads the pressure and air flow entering the system to decrease. Thus, the workability of the turbine through gas expansion is very poor. This phenomenon can also be observed from Fig.6 (e).

The system power is mainly from the fuel cell (as shown in Fig.6 (c)), achieving a higher efficiency. However, increasing rotational speed can alter this performance. Both air and

pressure rise with higher rotational speed, making the GT generate more power. When the increasing power level of GT is higher than that of the fuel cell,  $P_{GT}/P_{SOFC}$  begins to increase. It can also be seen that, for using WCG as fuel, the system efficiency is the highest, followed by GSG, CSG, and CWG successively.

#### 4.4 Analysis and Discussion

In different adjusting modes (Cases A, B and C), component operating characteristics and system performance can be extensively analyzed by comparing those results in Figs. 4, 5 and 6.

When the system is in variable load operation states, the compressor SM firstly increases and then decreases in Case A (see Fig.4 (a)), it keeps constant in Case B (see Fig. 5(a)), but it decreases steadily in Case C (see Fig. 6(a)). More interestingly, when the system operates in Case A, CSG makes the SM reach 11.69% at system maximum load of 118.90%, which is below the SM lower threshold of 12% required by Table 3 in [29]. In this case, the air in the compressor can yield intense pulsation and produce reverse flow, causing the blade to vibrate and even break. While for using other fuels, the SM is higher than 12%.

Although Case A and Case C make the variation trends of fuel cell working temperature differently, all voltages drop gradually and mean temperature gradients increase (see Figs. 4(b) and 6(b)). By contrast, in Case B, the cell voltage rises and the mean temperature gradient reaches a minimum with increasing system load (see Fig. 5(b)). The reason is that with a constant air flow rate, small fuel flow causes reformer temperature to be very low and consequently water gas shift reaction to play a major role. Therefore, heat is released, causing the reformer outlet temperature to increase, the temperature difference between both ends of the

fuel cell to decrease, and ultimately the mean temperature gradient decreases. On the contrary, with increasing fuel flow, the reformer temperature increases, and CH<sub>4</sub> reforming plays a major role. In this case, heat is absorbed, causing the reformer outlet temperature to decrease and the temperature difference **between** both ends of the fuel cell and the mean temperature gradient to increase. This phenomenon implies that the fuel cell inner temperature profile changes sharply in a variable load operation, which is a great challenge for selecting proper coefficient of thermal expansion of fuel cell materials.

In Case C, the fuel cell working temperature decreases to the designed value and then increases with rising system load. It is probably due to that when the fuel-air ratio is constant, low rotational speed will cause the pressure ratio and airflow entering the system to be very small, resulting in a decreasing enthalpy drop of adiabatic expansion in the turbine. Hence, high-temperature exhaust gas entering the system escalates the working temperature of heat exchanger and evaporator, and finally causes the fuel cell working temperature to increase. However, with increasing rotational speed, the pressure ratio and air entering the system rise gradually, and the enthalpy drop of adiabatic expansion in the turbine also increases, leading the temperature of turbine exhaust gas to decline. The consequence is that the reduction **in** the fuel cell working temperature. All three adjusting modes make the cell output power increase gradually with increasing system load, but the cell efficiency **varies** significantly. Case A and Case C cause the cell efficiency to decrease while Case B has an opposite effect on it. More interestingly, in Case B, the fuel cell outputs higher power when the system using CWG and CSG as fuel, but in Case C, the fuel cell efficiency can reach a maximum with WCG (see

Fig.6(c)).

In reforming process, both Case A and Case C inhibit  $\text{CH}_4$  reforming reaction, and promote water gas shift reaction, causing  $\text{S/C}_{\text{bv}}$  to increase gradually (see Figs. 4(d) and 6(d)). While, in Case B, the generation of carbon deposition in the reformer can be effectively suppressed, which leads to a decline in  $\text{S/C}_{\text{bv}}$  (see Fig. 5(d)). Meanwhile, in using all four types of biomass gases, all  $\text{S/C}_{\text{bv}}$  is higher than  $\text{S/C}$  limit value in Table 3 in [29], when the system is operated in load ranges of 17.45%~77.09%, 21.96%~88.44%, 17.19%~76.43%, and 23.13%~90.14%, respectively. This means that the water added in the reformer is less than that for avoiding carbon deposition. Hence, if the system operates for a long period, the reformer exit might be blocked or catalyst activity is reduced.

Case A can keep the TIT almost unchanged with increasing system load. The GT output power presents a peak value when using WCG and GSG, but this trend is not applicable to other two fuels (as shown in Fig.4(e)). Case B can make the GT output reach a maximum power (see Fig. 5(e)) when using CSG. The TITs present increasing trends in all four types of fuels. It is also important to note that TITs are less than 1023K constrained by the low threshold [29], when the system load is below 54.21%, 62.85%, 53.65%, and 64.16%, respectively. While TITs are higher than 1223K required in Table 3 in [29], when the system load is higher than 122.83%, 140.82%, 121.87%, and 143.50%, respectively. In practice due to over-temperature, some serious phenomenon would appear, such as turbine inlet material deformation or system performance degradation. Different from Cases A and B, Case C causes TIT first to decrease and then increase, and GT power to reach a peak value (see Fig. 6(e)).

Electric efficiency is an important parameter for evaluating the performance of the hybrid system. It can be seen from Figs. 4(f) and 6(f) that, Case A and Case C have a similar effect on the variation trend of system efficiency, both making it decline after reaching the designed value. While in Case B, system efficiency gradually increases but no peak value exists (see Figs.5(f)). More interestingly, when the system operates with these three adjusting modes using WCG as fuel, the system efficiency is highest among all four types of fuels.

Conclusively, the effect of different types of biomass gases on the variable load characteristics of the system in the three adjusting modes is summarized in Fig.7. As seen, in all three modes and all types of biomass gases, the maximum system efficiency can exceed 59%. In Case A and Case C, CWG and CSG can make system load change from 46% to 120%, but biomass gas fuel CSG may cause compressor surge in Case A. WCG and GSG can make the system load change from 40% to 103%, enabling it to present excellent operating performance. In Case B, although all types of biomass gases can lead the system to have a wider range of load adjustment, the system operating is much more complicated. When the system is in a light load operation, too low TIT or carbon deposition in the reformer could endanger the safe operation of the hybrid system. When the system is in heavy load condition, the turbine might suffer from over-temperature, leading to system unsafety. Hence, under normal and safe operations, the system load ranges are from 88.44% to 140.82% for CWG and CSG, and are 77.09%~122.83% and 76.43%~121.87% when using WCG and GSG. Therefore, in normal and safe cases, more attention should be paid to the matching between high gas flow and turbine flow characteristics.

Although the quantitative results are only applicable to the hybrid system established in this work, the research method and results have a guiding significance for system design and adjusting mode selection of other similar practical hybrid systems.

## 5. Conclusions

By using the model of an IT-SOFC/GT hybrid system, this paper investigates the effect of different types of biomass gases on the component operation and hybrid system load characteristics. It also discusses the relationship between fuel type and load adjusting modes. Through simulations and analysis, the following key points are observed.

1) When using WCG as design fuel, the small power system of 182.4kW has a high electric efficiency of 60.78%. If CWG and CSG replace the WCG, both  $S/C_{bv}$  and hybrid system output power are higher, but system efficiency decreases to 57.36% and 57.87%, respectively. When using GSG, both system power and efficiency are smaller than those of WCG.

2) Fuel type has a great effect on the component operation and system characteristics in various adjusting modes. In Case A, when using CWG and CSG, the operating characteristics of reformer and gas turbine can be improved and system load ranges are wider than those of other two fuels, but system efficiency declines. In Case B, when using WCG, the system efficiency is higher than that of other three fuels. The effect of CWG and CSG on operating characteristics of the reformer is not obvious. In Case C, although the CWG and CSG degrade fuel cell performance, they can improve the reforming characteristics of the reformer and workability of the gas turbine.



3) Different fuels should be matched with appropriate adjusting modes to ensure that the system presents excellent performance. With the three load adjusting modes, all types of biomass gases can make the maximum efficiency of the hybrid system exceed 59%. If a high efficiency (for example 62.73%) and a wide range of load adjustment are required by users, Case B is more appropriate with using fuels like WCG and GSG. When users require the system to have higher efficiency and low load, Case A is more suitable. With fuels like CWG and CSG, Case C is desirable for good system safety performance and lower load adjusting.

## **6. Acknowledgments**

The research is supported by National Natural Science Foundation of China under grant No.51376123, 863 Program of China (No.2014AA052803) and The Engineering and Physical Sciences Research Council-EPSRC (EP/M000141/1).

## 7. References

- [1] Fuel Cell Handbook. U.S. Department of Energy, Office of Fossil Energy, National Energy Technology Laboratory, November 2004.
- [2] Kaneko T, Brouwer J, Samuelsen G.S. Power and temperature control of fluctuating biomass gas fueled solid oxide fuel cell and micro gas turbine hybrid system. *J Power Source* 2006; 160: 316–325.
- [3] Bang-Møller C, Rokni M. Thermodynamic performance study of biomass gasification, solid oxide fuel cell and micro gas turbine hybrid systems. *Energy Convers. Manage* 2010; 51: 2330-2339.
- [4] Bang-Møller C, Rokni M, Elmegaard B. Exergy analysis and optimization of a biomass gasification, solid oxide fuel cell and micro gas turbine hybrid system. *Energy* 2011; 36: 4740-4752.
- [5] Toonssen R, Aravind P.V, Woudstra N, H.M. Verkooijen A. Alternative system designs of biomass gasification SOFC/GT hybrid systems. *Int J Hydrogen Energy* 2011;36:10414-10425.
- [6] Karellas S, Karl J, Kakaras E. An innovative biomass gasification process and its coupling with micro turbine and fuel cell systems. *Energy* 2008;33:284–291.
- [7] Facchinetti E, Gassner M, Favrat D. Process integration and optimization of a solid oxide fuel cell-gas turbine hybrid cycle fueled with hydrothermally gasified waste biomass. *Energy* 2012; 41:408-419.
- [8] Zhao Y, Sadhukhan J, Lanzini A, Brandon N, Shah N. Optimal integration strategies for a syngas fuelled SOFC and gas turbine hybrid. *J Power Source* 2011; 196: 9516-9527.

- [9] Bakalis D P, Stamatis A G. Incorporating available micro gas turbines and fuel cell: Matching considerations and performance evaluation. *Appl Energy* 2013; 103: 607–617.
- [10] Zabihian F, Fung A S. Performance analysis of hybrid solid oxide fuel cell and gas turbine cycle: Application of alternative fuels. *Energy Convers. Manage* 2013; 76: 571–580.
- [11] Sucipta M, Kimijima S. Biomass Solid Oxide Fuel Cell-Microgas Turbine Hybrid System: Effect of Fuel Composition. *J Fuel Cell Sci Tech* 2008;5.
- [12] Zhang X, Wang Y, Liu T, Chen J. Theoretical basis and performance optimization analysis of a solid oxide fuel cell-gas turbine hybrid system with fuel reforming. *Energy Convers. Manage* 2013; 61:1102–1109.
- [13] Marsano F, Magistri L, Bozzolo M, Tarnowski O. Influence of fuel composition on solid oxide fuel cell hybrid system layout and performance. *ASME Turbo Expo* 2004: 533-540.
- [14] Santin M, Traverso A, Magistri L. Liquid fuel utilization in SOFC hybrid systems. *Appl Energy* 2009; 86: 2204-2212.
- [15] Santin M, Traverso A, Magistri L, Massardo A. Thermoeconomic analysis of SOFC-GT hybrid systems fed by liquid fuels. *Energy* 2010; 35: 1077-1083.
- [16] Maréchal F, Leuenberger S, Membrez Y, Bucheli O, Favrat D. Process flow model of solid oxide fuel cell system supplied with sewage biogas. *J Power Sources* 2004; 131:127-141.
- [17] Zabihian F, Fung A S. Performance analysis of hybrid solid oxide fuel cell and gas turbine cycle (part I): Effects of fuel composition on output power. *J Energy Inst* 2014; 87: 18-27.
- [18] Zabihian F, Fung A S. Performance analysis of hybrid solid oxide fuel cell and gas turbine cycle (part II): Effects of fuel composition on specific work and efficiency. *J Energy Inst* 2014;

87: 28-34.

[19] Sucipta M, Kimijima S, Song T W, Suzuki K. Biomass solid oxide fuel cell-microgas turbine hybrid system: Effect of fuel composition. *J Fuel Cell Sci Tech* 2008; 5:1-8.

[20] Sucipta M, Kimijima S, Suzuki K. Performance analysis of the SOFC–MGT hybrid system with gasified biomass fuel. *J Power Sources* 2007; 174: 124-135.

[21] Rokni M. Thermodynamic analysis of SOFC (solid oxide fuel cell)-Stirling hybrid plants using alternative fuels. *Energy* 2013; 61: 87-97.

[22] Harun N F, Tucker D, Adams T A. Fuel Composition Transients in Fuel Cell Turbine Hybrid for Polygeneration Applications. *J Fuel Cell Sci Tech* 2014; 11: 1-8.

[23] Fernandes A, Woudstra T, Aravind P V. System simulation and exergy analysis on the use of biomass-derived liquid-hydrogen for SOFC/GT powered aircraft. *Int J Hydrogen Energy* 2015; 40: 4683-4697.

[24] Ma S, Wang J, Yan Z, Dai Y, Lu B. Thermodynamic analysis of a new combined cooling, heat and power system driven by solid oxide fuel cell based on ammonia–water mixture. *J Power Sources* 2011; 196: 8463-8471.

[25] Caliandro P, Tock L, Ensinas A V, Marechal F. Thermo-economic optimization of a solid oxide fuel cell-gas turbine system fuelled with gasified lignocellulosic biomass. *Energy Convers. Manage* 2014; 85: 764-773.

[26] Li Y, Weng Y. Performance study of a solid oxide fuel cell and gas turbine hybrid system designed for methane operating with non-designed fuels. *J Power Source* 2011;196 ;3824-3835.

[27] Milewski J, Miller A, Sałaciński J. Off-design analysis of SOFC hybrid system. *Int J*

Hydrogen Energy 2007; 32: 687 – 698.

[28] Calise F, Palombo A, Vanoli L. Design and partial load exergy analysis of hybrid SOFC-GT power plant. J Power Source 2006.;158:225–244.

[29] Lv X, Weng Y. Effect of operating parameters on a hybrid system of intermediate-temperature solid oxide fuel cell and gas turbine. Energy 2015; 91: 10-19.

[30] Lv X, Weng Y. Safety Analysis of a SOFC/GT Hybrid System Fueled With Gasified Biomass. J Fuel Cell Sci Tech 2015;12:011008-1-011008-6.

[31] Aguiar P, Adjiman C S, Brandon N P. Anode supported intermediate temperature direct internal reforming solid oxide fuel cell. I: Model-based steady-state performance. J Power Source 2004.;138:120-136.

[32] Wang Y, Yoshiba F, Kawase M, Watanabe T. Performance and effective kinetic models of methane steam reforming over Ni/YSZ anode of planar SOFC. Int J Hydrogen Energy 2009;34: 3885-3893.

[33] Liu A, Weng Y. Performance analysis of a pressurized molten carbonate fuel cell/micro-gas turbine hybrid system. J Power Source 2010;195: 204–213.

[34] Yao Z, Weng Y. Characteristic analysis of a fuel cell and gas turbine hybrid system utilizing biomass syngas[D]. Shanghai Jiao Tong University. 2012( In Chinese ).

[35] Barelli L, Bidini G, Ottaviano A. Part load operation of SOFC/GT hybrid systems: Stationary analysis. Int. J Hydrogen Energy 2012; 37: 16140-16150.

[36] Komatsu Y, Kimijima S, Szmyd J.S. Performance analysis for the part-load operation of a solid oxide fuel cell-micro gas turbine hybrid system. Energy 2010; 35; 982–988.

- [37] Yin. J, Weng Y, Su S. Investigation on performance of a lean-burn catalytic combustion micro gas turbine system[D]. Shanghai Jiao Tong University PhD. 2010( In Chinese ).
- [38] Liu A, Weng Y. Numerical simulation of fuel cells/gas turbine hybrid power system and catalytic combustion experiment study[D]. Shanghai Jiao Tong University PhD. 2009( In Chinese ).
- [39] Li Y, Weng Y. Off-design analysis and experiment study of high temperature fuel cell/gas turbine hybrid system[D]. Shanghai Jiao Tong University PhD. 2011( In Chinese ).

## 8. Nomenclature

Nomenclature	
$M$	mole flow rate(kg s <sup>-1</sup> )
$n_i$	composition $i$ mole flow rate(mol s <sup>-1</sup> )
$K_1$	CH <sub>4</sub> reforming reaction equilibrium constant
$K_2$	water gas shift reaction equilibrium constant
$LHV$	lower heating value(kJ mol <sup>-1</sup> )
$P_{SOFC}$	SOFC output power(kW)
$P_T$	turbine output power(kW)
$P_{C,air}$	air compressor consumption power(kW)
$P_{C,fuel}$	fuel compressor consumption power(kW)
$P_{P,air}$	water syringe pump consumption power(kW)
$\eta_{DC/AC}$	DC/AC inverter efficiency (%)
$\eta_g$	electric generator(%)
$\eta_m$	GT mechanical efficiency (%)
$\eta_e$	electric motor efficiency(%)
$y_i$	composition $i$ mole fraction(%)
$x$	CH <sub>4</sub> consumption mole in reforming reaction
$y$	CO consumption mole in reforming reaction
$U_f$	fuel utilization
$S/C$	ratio of steam to CH <sub>4</sub> , CO, and CO <sub>2</sub>
$S/C_{bv}$	boundary value of the S/C ratio
Abbreviation	
TIT	turbine inlet temperature
SM	surge margin
GT	gas turbine
IT-SOFC	intermediate-temperature solid oxide fuel cell
MTG	mean temperature gradient
WCG	wood chip gas
CWG	cotton wood gas
GSG	grape seed gas
CSG	corn stalk gas
CC	catalytic combustor
HE	heat exchanger
CD	carbon deposition
HT	higher temperature
LT	lower temperature



Figure Caption List:

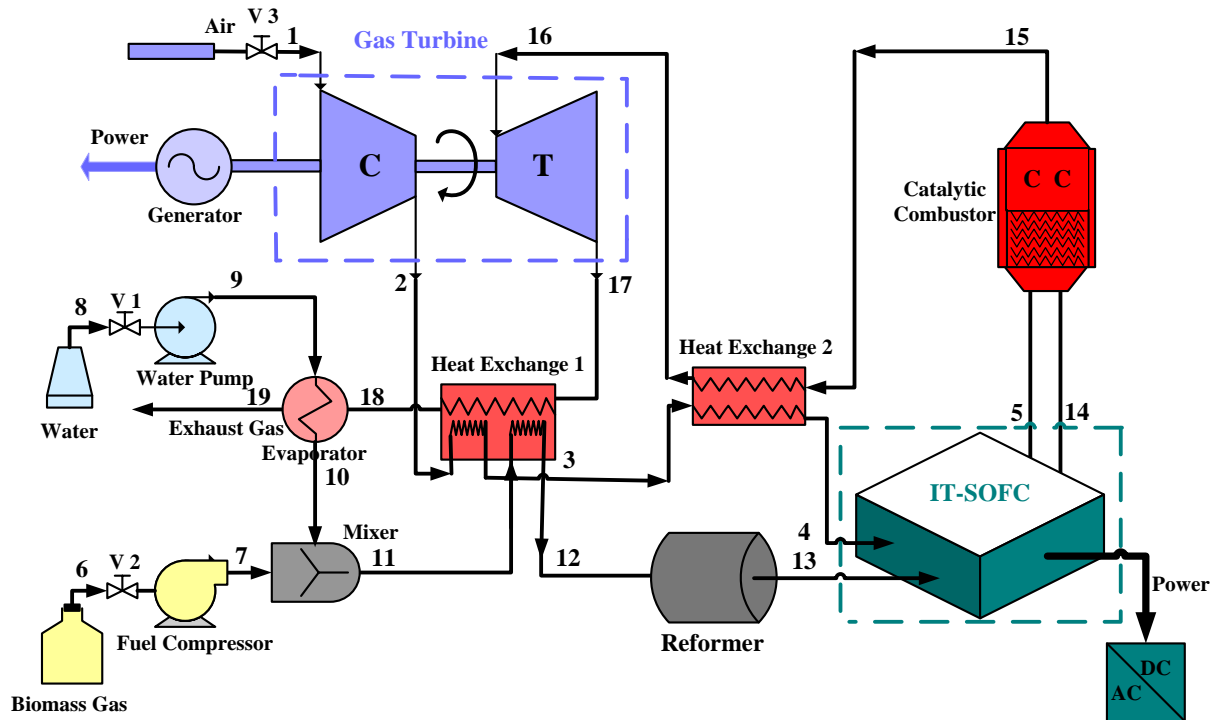


**Fig. 1** The schematic of the IT-SOFC/GT hybrid system.

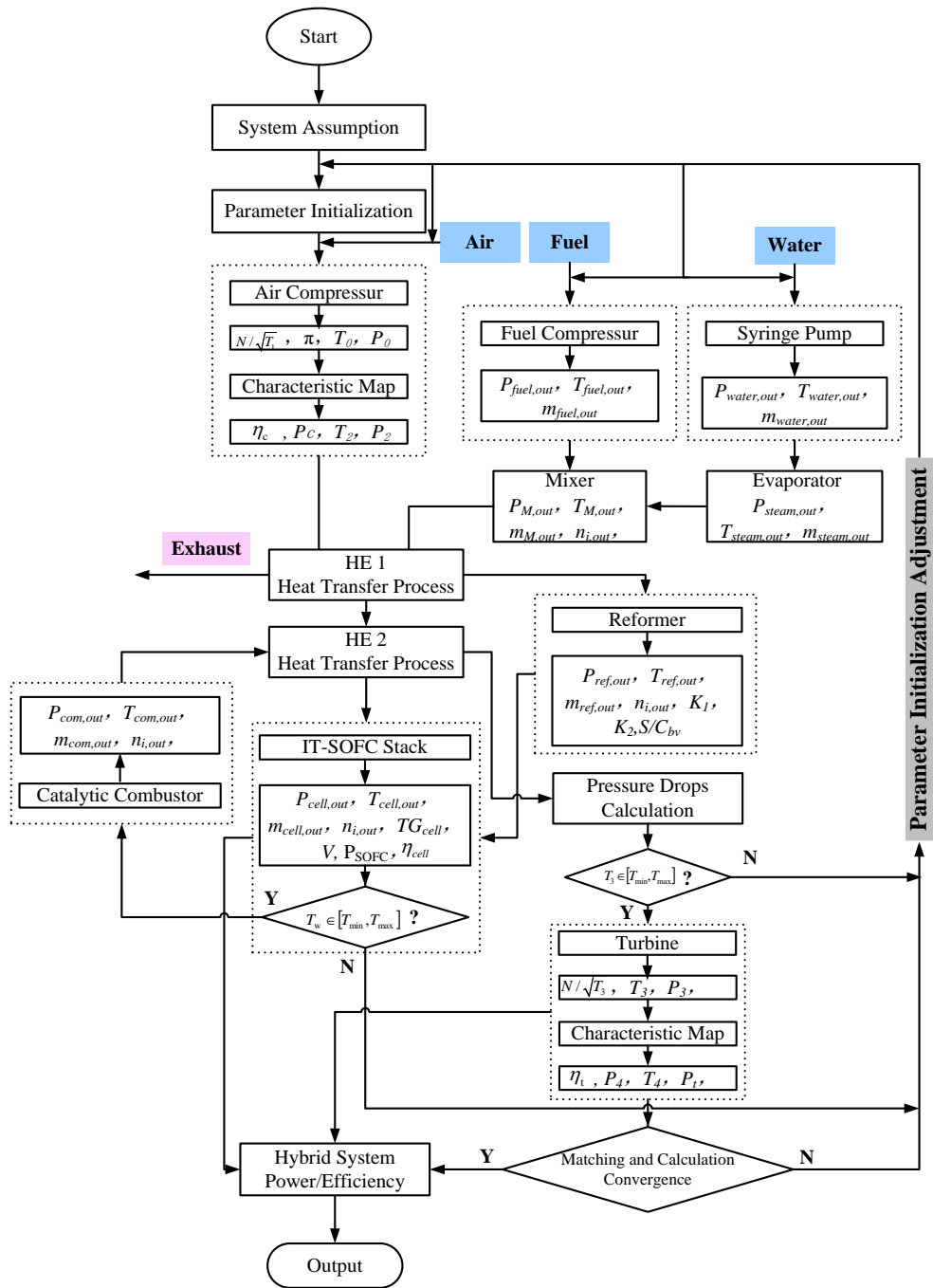


Fig. 2 Circulation flowchart of the IT-SOFC/GT.

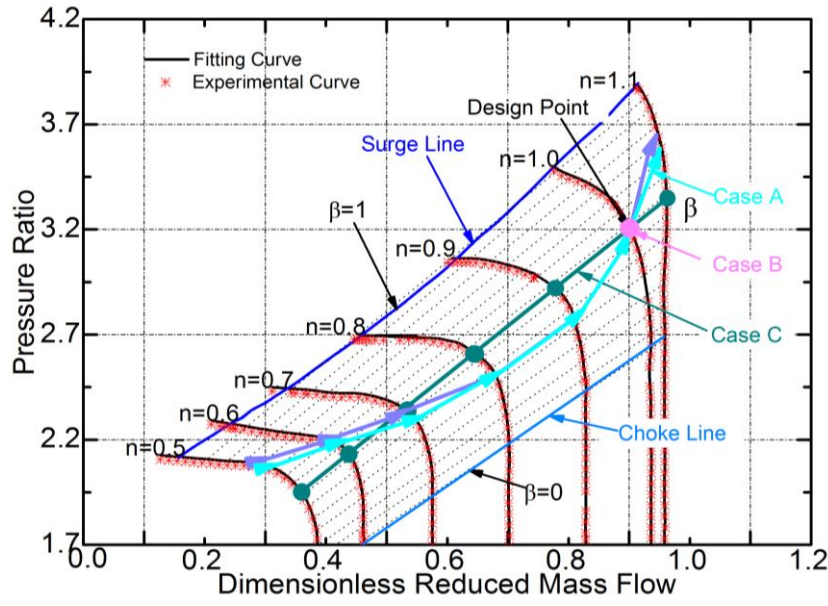


Fig. 3 Gas turbine operating trajectory map.

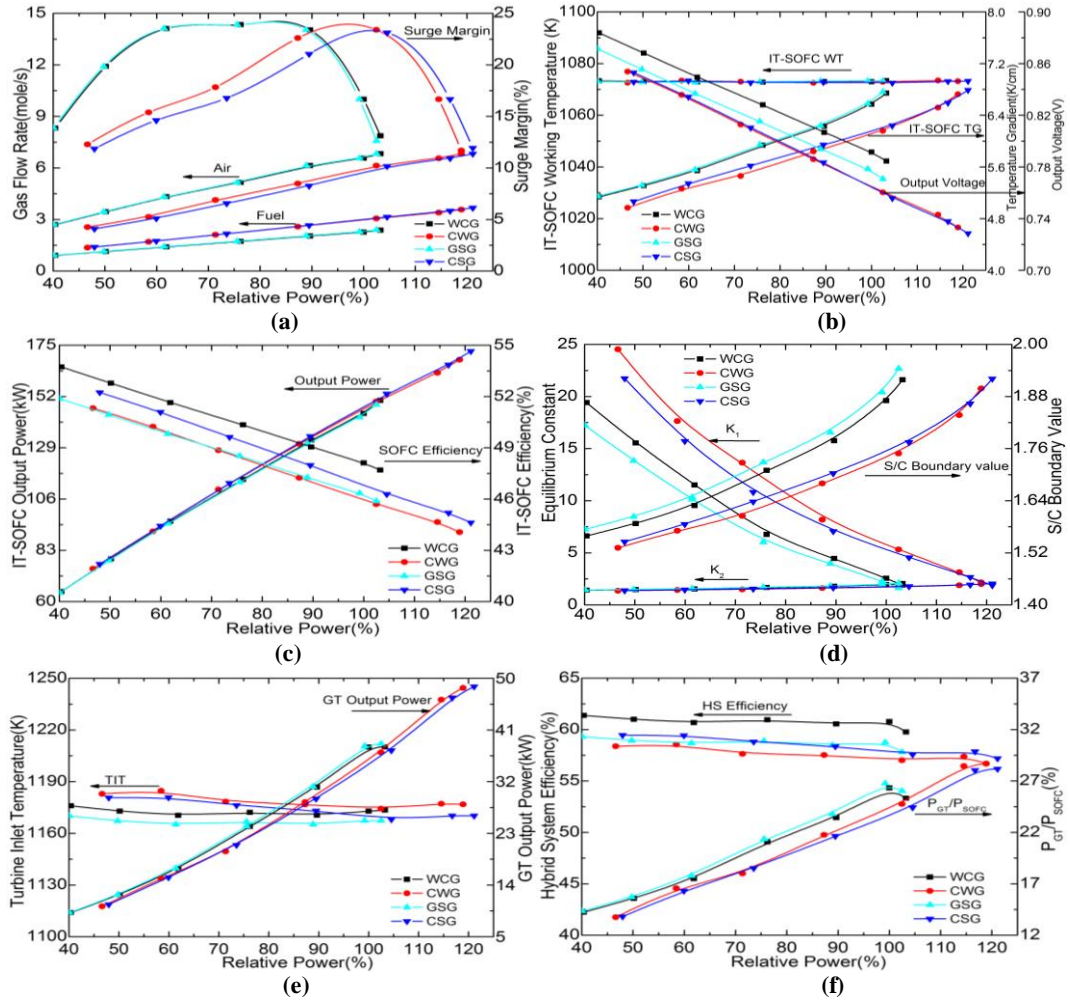


Fig. 4 The effect of different inlet fuels on the load characteristics of the hybrid system in Case

A.

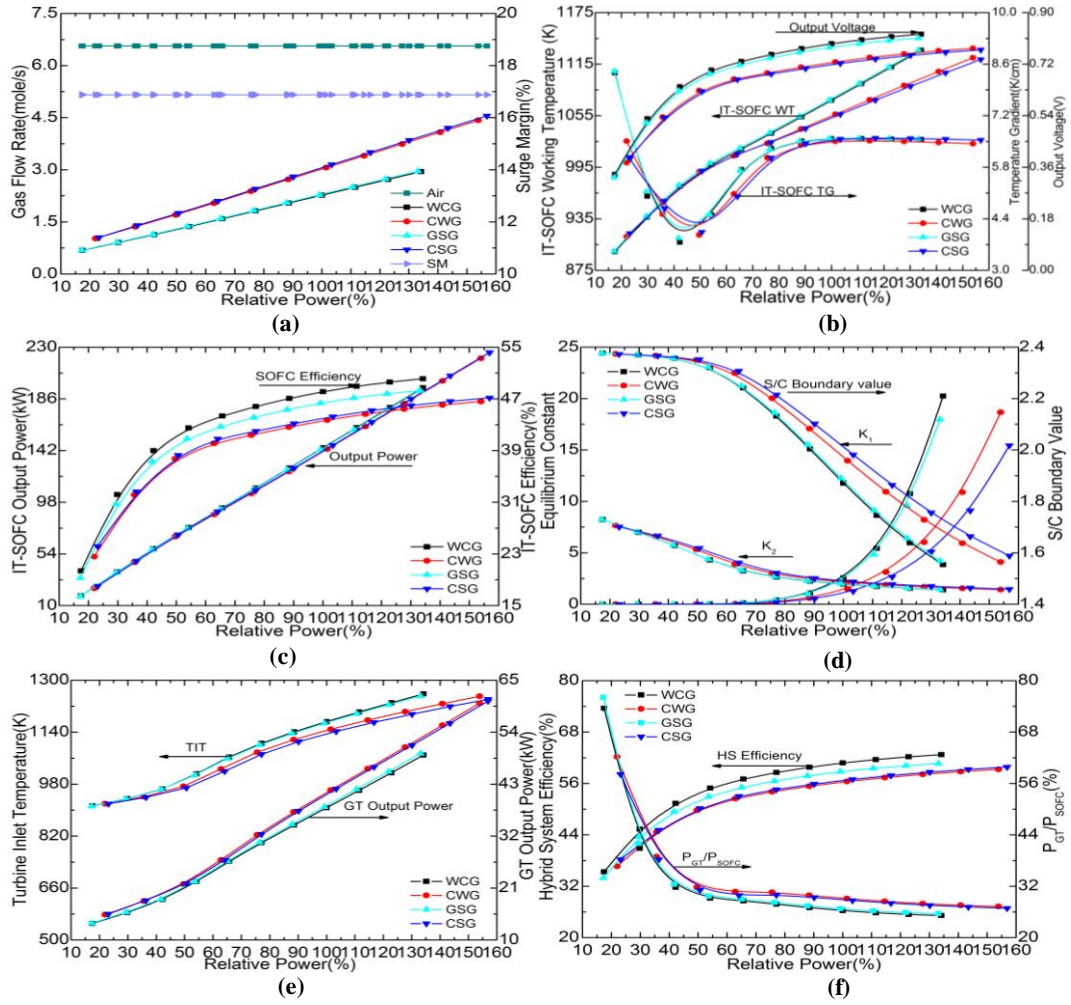


Fig. 5 The effect of different inlet fuels on the load characteristics of the hybrid system in Case

B.

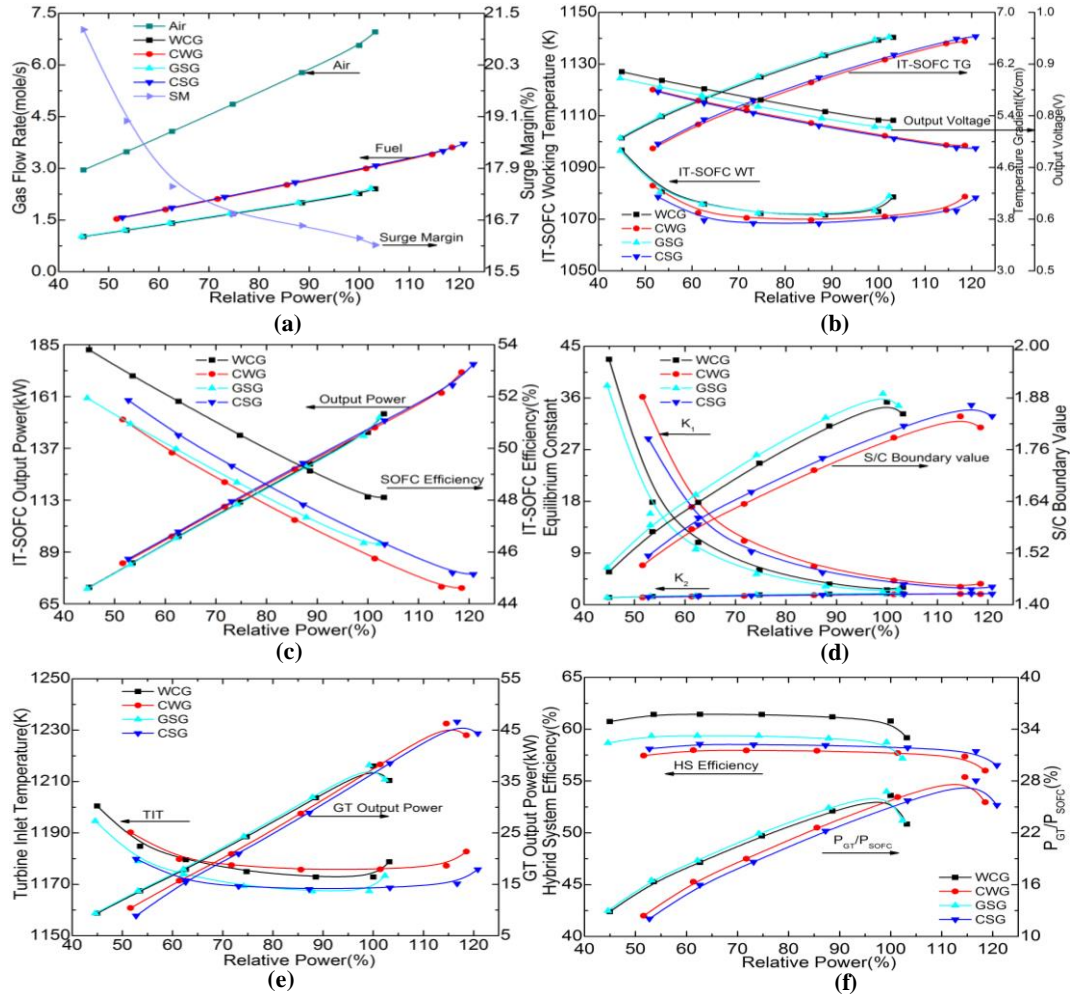


Fig. 6 The effect of different inlet fuels on the load characteristics of the hybrid system in Case

C.

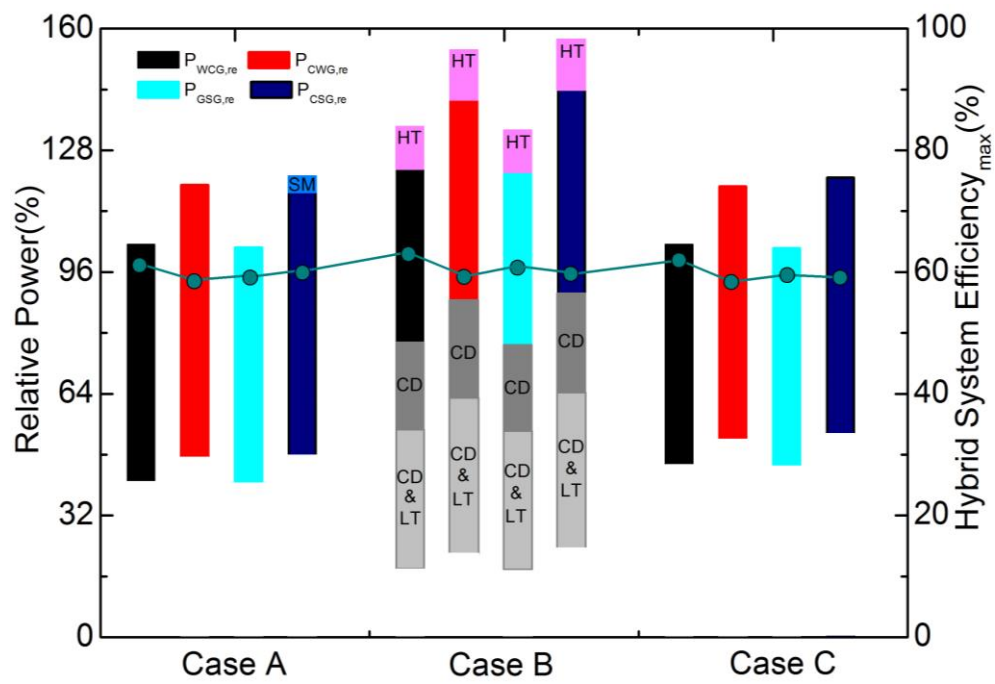


Fig. 7 Results comparison when using different types of fuels.

Table Caption List:

Table. 1 Composition and lower heating value of different gasified biomass.

Type	CH <sub>4</sub> [%]	H <sub>2</sub> [%]	CO[%]	CO <sub>2</sub> [%]	N <sub>2</sub> [%]	C <sub>n</sub> H <sub>m</sub> [%]	LHV[MJ/Nm <sup>3</sup> ]
WCG	4.34	23.03	15.04	17.75	39.81	0.00	7.79
CSG	1.90	12.20	21.40	13.00	51.50	0.00	5.33
CWG	1.90	11.50	22.70	11.60	51.30	1.00	5.39
GSG	4.00	17.00	22.00	13.00	42.00	2.00	7.41

Table. 2 Performance of the IT-SOFC/GT Hybrid system.

Type	WCG $U_f=75\%$	CWG $U_f=60\%$	GSG $U_f=75\%$	CSG $U_f=60\%$
Fuel flow rate/mol/s	2.269	3.403	2.28	3.502
IT-SOFC current density/ A/m <sup>2</sup>	5000	6000	5025	6175
IT-SOFC working temperature/K	1073	1073	1073	1073
IT-SOFC MTG/ K/cm	6.571	6.518	6.581	6.592
S/C boundary value	1.87	1.84	1.89	1.86
IT-SOFC voltage/V	0.79	0.74	0.78	0.74
IT-SOFC power/kW	144.4	162.6	142.7	166.2
TIT /K	1173	1171	1167	1170
Gas flow rate/ kg/s	0.2747	0.3251	0.2794	0.3293
GT power/kW	38.01	46.28	38.19	46.62
Air compressor consumption/kW	27.48	27.48	27.48	27.48
Fuel compressor consumption/kW	7.929	13.1	8.3	13.51
Syringe pump consumption /kW	0.012	0.018	0.013	0.019
Hybrid system power/kW	182.4	208.9	180.9	212.9
Hybrid System efficiency/%	60.78	57.36	58.74	57.87